Clinical Cancer Research

Cervical Cancer Stem Cells Selectively Overexpress HPV Oncoprotein E6 that Controls Stemness and Self-Renewal through Upregulation of HES1

Abhishek Tyagi[1,2,3], Kanchan Vishnoi[2], Sutapa Mahata[2], Gaurav Verma[2], Yogesh Srivastava[2], Shashank Masaldan[2], Bal Gangadhar Roy[4], Alok C. Bharti[2,5], and Bhudev C. Das[1,3]

Abstract

Purpose: Perturbation of keratinocyte differentiation by E6/E7 oncoproteins of high-risk human papillomaviruses that drive oncogenic transformation of cells in squamocolumnar junction of the uterine cervix may confer "stem-cell like" characteristics. However, the crosstalk between E6/E7 and stem cell signaling during cervical carcinogenesis is not well understood. We therefore examined the role of viral oncoproteins in stem cell signaling and maintenance of stemness in cervical cancer.

Experimental Design: Isolation and enrichment of cervical cancer stem–like cells (CaCxSLCs) was done from cervical primary tumors and cancer cell lines by novel sequential gating using a set of functional and phenotypic markers (ABCG2, CD49f, CD71, CD133) in defined conditioned media for assessing sphere formation and expression of self-renewal and stemness markers by FACS, confocal microscopy, and qRT-PCR. Differential expression level and DNA-binding activity of Notch1 and its downstream targets in CaCxSLCs as well as silencing of HPVE6/Hes1 by siRNA was evaluated by gel retardation assay, FACS, immunoblotting, and qRT-PCR followed by *in silico* and *in vivo* xenograft analysis.

Results: CaCxSLCs showed spheroid-forming ability, expressed self-renewal and stemness markers Oct4, Sox2, Nanog, Lrig1, and CD133, and selectively overexpressed E6 and HES1 transcripts in both cervical primary tumors and cancer cell lines. The enriched CaCxSLCs were highly tumorigenic and did recapitulate primary tumor histology in nude mice. siRNA silencing of HPVE6 or Hes1 abolished sphere formation, downregulated AP-1-STAT3 signaling, and induced redifferentiation.

Conclusions: Our findings suggest the possible mechanism by which HPVE6 potentially regulate and maintain stem-like cancer cells through Hes1. *Clin Cancer Res; 22(16); 4170–84. ©2016 AACR.*

Introduction

Persistent infection of high-risk human papillomaviruses (HR-HPV) is causally linked to the development of cervical cancer (1, 2). Despite effective cervical cancer screening programs and development of successful prophylactic HPV vaccines (3), available therapeutic options to treat and cure HPV-induced cervical cancers are minimal. There is often recurrence of lesions with selection of drug-resistant tumor clones with stem cell–like properties resulting in treatment failure (4). Although persistent infection of HPV and its integration in host genome is an essential perquisite for the progression of cervical cancer (5), the events that precede to provide niche for establishment of viral infection and the mechanisms thereof in some initial cells currently referred to as cancer stem cells (CSC) or tumor-initiating cells are poorly understood (6). Most importantly, the role of HPV infection and/or viral oncoproteins in these CSCs is unknown.

It is hypothesized that a small population of cells termed as "reserve cells" in transformation zone (TZ) of cervix are the targets of HPV infection (7). Reports suggest preferential physical interaction of the virus with squamocolumnar junction (SCJ) in TZ that forms basal/reserve cells with stem cell properties (8). These observations along with technological advancements in identification of CSCs using established phenotypic and functional markers have facilitated identification and characterization of cervical CSCs from primary tumors (7, 9) and cervical cancer cell lines (10). The cell lines, SiHa (HPV16$^+$) and HeLa (HPV18$^+$) constitutively express markers that closely resemble SCJ cells (8) thus making them a suitable experimental model for investigation of cervical CSCs in greater detail. Earlier studies on cervical CSCs

[1]Stem Cell and Cancer Research Laboratory, Amity Institute of Molecular Medicine and Stem Cell Research, Amity University Campus, Noida, Uttar Pradesh, India. [2]Division of Molecular Oncology, Institute of Cytology & Preventive Oncology (ICMR), Noida, Uttar Pradesh, India. [3]Molecular Oncology Laboratory, B.R. Ambedkar Centre for Biomedical Research (ACBR), University of Delhi, Delhi, India. [4]Institute of Nuclear Medicine and Allied Sciences, DRDO, Delhi, India. [5]Molecular Oncology Laboratory, Department of Zoology, University of Delhi, Delhi, India.

Note: Supplementary data for this article are available at Clinical Cancer Research Online (http://clincancerres.aacrjournals.org/).

Current address for B.C. Das: Stem Cell and Cancer Research Laboratory, Amity Institute of Molecular Medicine and Stem Cell Research, Amity University, Noida, Uttar Pradesh 201313, India; and current address for A.C. Bharti, Molecular Oncology Laboratory, Department of Zoology, University of Delhi, Delhi 110007, India.

Corresponding Authors: B.C. Das, Stem Cell and Cancer Research Laboratory, Amity Institute of Molecular Medicine and Stem Cell Research, Amity University, Sector-125, Noida, Uttar Pradesh 201313, India. Phone: 91-120-4586855; Fax: 91-120-4392114; E-mail: bcdas@amity.edu; and A.C. Bharti, Molecular Oncology Laboratory, Department of Zoology, University of Delhi, Delhi 110007, India. E-mail: alokchandrab@yahoo.com

doi: 10.1158/1078-0432.CCR-15-2574

Translational Significance

A novel triple gating method has been developed using phenotypic and functional markers for identification and enrichment of cervical cancer stem cells. HPVE6 oncogene, which causes cervical cancer in women, is shown for the first time to be involved in self-renewal and maintenance of stemness in cervical cancer stem cells through Hes1 expression. These cells form highly tumorigenic xenografts that recapitulate primary tumor morphology. It demonstrates that oncogenic viruses such as HPV can share mechanisms of cellular reprogramming along with carcinogenesis through modulation of signaling pathways associated with the induction of stemness, which provides an opportunity for survival of these cancer cells through acquired drug resistance and recurrence. Therefore, HPVE6 could serve as an important drug target for therapeutic intervention of chemo-radioresistant cervical cancer stem cells that cause tumor relapse and metastasis.

were primarily focused on their role in chemo- or radioresistance and metastasis but lacked information on the role of the primary causative agent HPV in cervical CSC function and signaling.

High-risk HPVs are known to code for two well-characterized viral oncoproteins E6 and E7 that functionally interfere with the host cell cycle by interacting with its key regulatory proteins p53 and Rb, respectively (11, 12). However, the role of E6 and E7 in regulation of cervical CSC function and their signaling is not known. Some early studies indicate involvement of E6/E7 in downmodulation of Notch signaling (13, 14) that controls stemness (15). Apart from Notch1, a quiescent cell marker, Lrig1 is specifically expressed in epithelial stem cells (16). This prompted us to investigate the role of HPV particularly of E6 and E7 oncoproteins in signaling and maintenance of cervical CSCs. For this, we developed an efficient triple gating method for isolating and enriching cervical CSCs and molecularly dissected the role played by HPV E6 in the maintenance of tumor phenotype as well as stemness in cervical stem cells.

Materials and Methods

Cell lines and cell culture

Human cervical cancer cell lines SiHa (HPV16$^+$), HeLa (HPV18$^+$), and C33a (HPV$^-$) were obtained from the ATCC. The cells were maintained using the DMEM (Sigma Aldrich) medium containing 10% heat-inactivated FCS (Sigma Aldrich) at 37 °C in a humidified atmosphere containing 5% CO_2.

Establishment of primary tissue culture

A total of 10 cervical tumor tissue specimens were collected in dissociated balanced salt solution (DBSS) containing antibacterial/antimycotic agents from the department of Gynecological Oncology in Lok Nayak Jai Prakash Narayan Hospital (New Delhi, India). Written informed consent was obtained from patients and a part of samples taken for diagnostic purposes was used for the study as approved by Institutional Ethics Committee of Dr. B.R. Ambedkar Center for Biomedical Research (ACBR), University of Delhi (Delhi, India). Primary tissue culture from cervical tumor tissue was established as described by Turin and colleagues (17). The purified primary tissue cultures under low-adhesion condition formed tumorspheres and were used for isolation, characterization of primary cervical cancer stem-like cells (pCaCxSLC) by novel sequential triple gating and generating tumor xenograft in nude mice.

Isolation and characterization of CSCs from cervical primary tissue culture and cell lines by side population analysis

Side population (SP) analysis was performed as described previously (18). Briefly, 1×10^6 cells from primary tissue culture or cell lines were incubated at 37 °C for 30 minutes with or without Fumitremorgin C (FTC; Alexis Biochemical) and then stained with dye cycle violet (DCV; 10 μmol/L; Life Technologies) for 90 minutes. The cells were then treated with 7-aminoactinomycin D (7-AAD; BD Biosciences) to discriminate viable cells. Data were collected on FACSAriaIII cell sorter (BD Biosciences) and analyzed using FlowJo (TreeStar). For SP and Non-Side Population (NSP) gating, we ran the experiment in two parallel setup one with and other without 10 μmol/L FTC as described by Telford and colleagues (18). In brief, cells were distinguished from debris on flow cytometer based on forward scatter (FSC) and side scatter (SSC). Doublets and aggregates were gated out based on SSC area (SSC-A) versus height (SSC-H) to ensure that a detected signal arises from single cells. Dead cells were recognized by their strong positivity for 7-AAD. The DCV fluorescence was excited with violet laser at 407 nm and was measured with 450/40BP (DCV-Blue) and 565LP (DCV-Red) filters and was displayed as dual fluorescence dot plot on a linear scale in presence or absence of FTC. Later, a gate drawn on the limit of DCV^{dim} staining during FTC inhibition included fewer SPs cells recognized as a dim tail extending from main population with a characteristic low fluorescence, whereas intense fluorescence signals of bulk population were defined as NSP cells (DCV^{bright}). Finally, for sorting, DCV^{dim} (SP) and DCV^{bright} (NSP) cells in combination with fluorescent-labeled specific antibodies were analyzed for stem cell marker expression.

Cervicosphere culture

Cervicosphere cultures were established as described by Dontu and colleagues with minor modifications (19). In brief, 1×10^4 cells/well were seeded on 6-well plates (Corning) precoated with 1.2% Poly-HEMA (Sigma-Aldrich) in defined conditioned medium (DCM) consisting of K-SFM (Invitrogen) supplemented with 10 ng/mL basic fibroblast growth factor (BD Biosciences), 10 ng/mL EGF (Sigma Aldrich) and B27 (Invitrogen). Sphere-forming efficiency (SFE) was calculated using the procedure described earlier (20). Subsequently, secondary and tertiary cervicospheres were generated by culturing in 1.2% Poly-HEMA precoated 6-well plates.

Determination of physical state of HPV16 DNA

Determination of physical state of viral DNA in HPV16$^+$ CINI/II, CINIII/IV cervical cancer lesions and primary xenograft was performed by the method described previously (21).

Quantitative real-time PCR

Quantitative real-time PCR was performed as described previously using a Bio-Rad iCycler (22). Results were normalized to the housekeeping gene *GAPDH*. Primer sets are listed in Supplementary Table S1.

Immunoblotting

Immunoblot analysis was performed for different cell phenotypes by the method described previously (23). The following primary antibodies (Santa Cruz Biotechnology) were used: Rb (IF-8), p53 (DO-1), HPV16/18E6 (C1P5), HPV16/18E7 (TVG710Y), Notch-1 (C-20), Hes1 (H-20), STAT3 (F-2), pSTAT3 (B-7), cFos (H-125), cJun (N), Ki-67 (H-300), and β-actin (C-11) and ABCG2 (BD Pharmingen), Nanog (N-17, BD Pharmingen).

Flow cytometry analysis and sorting

For flow cytometry analysis, cell suspension (1×10^5) obtained after enzymatic dissociation of primary and secondary cervicospheres were stained with anti-CD49f-FITC (GoH3; BD Pharmingen), anti-CD71-APC (M-A712; BD Pharmingen), and/or anti-CD133-PE for 60 minutes at 4°C in staining buffer (2% BSA in PBS). Corresponding isotypes were used as control. Cells were washed in PBS, centrifuged, and finally resuspended in 300-μL analysis buffer (1% BSA/2 mmol/L EDTA in PBS). For FACS sorting, 1×10^6 cells were incubated with anti-CD49f-FITC, anti-CD71-APC, and/or anti-CD133-PE, and were finally resuspended in 500-μL analysis buffer. The dead cells and debris were excluded after 7-AAD staining (Invitrogen). Data were collected on FACSAriaIII cell sorter (BD Biosciences) and analyzed using FlowJo software (TreeStar).

Electrophoretic mobility shift assay

Electrophoretic mobility shift assay (EMSA) was performed as described previously (23). Briefly, 10 μg of nuclear extract was incubated with γ-^{32}P-radiolabeled CSL-oligonulceotide (5′-GAAAGTTACTGTGGGAAAGAA-3′; ref. 24) for 30 minutes in 25 μL of reaction buffer. For the competition assay, 100× molar excess of unlabeled oligo (CSL) and nonspecific oligo (Oct-1) was added. Protein–DNA complexes were resolved in 6% nondenaturing polyacrylamide gel (crosslinking ratio, 29:1) and exposed to phosphorimager (Bio-Rad Laboratories). For the supershift assay, 2 μg nuclear extracts in reaction buffer were incubated with indicated antibodies for 60 minutes at room temperature before the addition of radiolabeled probe (γ-P^{32}) and electrophoresis.

Confocal imaging and image analysis

Staining of about 10–20 cervicospheres was done in uncoated chamber slide (Corning) as described by Weiswald and colleagues (25). A Leica TCS SP5 confocal microscope was used to view the immunofluorescence. The 488, 594, or 633 nm laser lines were used for excitation of the fluorophores, whereas emissions were collected by specific band pass filters. DAPI was used as a nuclear stain and Fluoromount as an antifade agent.

Cell-cycle analysis

Cell-cycle analysis was done using flow cytometry. Cells (1×10^5) were fixed in ice-cold 70% ethanol, incubated overnight at −20°C and stained with PI/RNAse solution (BD Biosciences) for 15 minutes at 37 °C. Cell-cycle analysis was performed using FACSAriaIII cell sorter and cell percentages in each phase of the cell cycle were analyzed using FlowJo software.

Cell proliferation assay

Cell proliferation was assessed by MTT and clonogenic assays. MTT assay was performed on days 3, 7, and 10 using the method described by Mosmann (26). Clonogenic assay was performed as described by Hamburger and Salmon (27). The colonies were stained with crystal violet and microscopically counted.

β-Galactosidase staining for cells undergoing senescence

Senescence assay was performed as described by Debacq-Chainiaux (28). Briefly, cells/cultures were washed with ice-cold PBS, fixed in 0.2% glutaraldehyde for 5 minutes at room temperatures and resuspended in 1 mg/mL X-Gal buffer and incubated in dark for 12 to 14 hours. The cells were viewed and counted under a phase contrast microscope.

RNA interference

RNA interference assay was done as described previously (29). Briefly, 2.5×10^3 cells cultured to 40% confluence were transfected with either 20 nmol/L HPV16E6 or Hes1 siRNAs (Santa Cruz Biotechnology), or scrambled siRNAs using RNAiMax (Invitrogen) following manufacturer's protocol. siRNA-treated cells were either incubated for 48 hours at 37 °C in a CO_2 incubator for mRNA expression and protein extraction or for 10 days to assess cervicosphere-forming ability.

Cervical cancer cell line and primary tissue culture xenografts

All animal experiments were approved by Institutional Animal Ethics Committee of Institute of Nuclear Medicine and Allied Sciences (Defence Research and Development Organisation, New Delhi, India) and ACBR, University of Delhi (Delhi, India). Female athymic nude mice at 8–10 weeks of age were made into five groups as in Supplementary Table S2. The tumor sizes were measured using vernier calipers biweekly and tumor volume (mm^3) was calculated using the standard formula: $(L \times W^2)/2$. Each mouse was euthanized when the diameter of the tumors reached approximately 1.0 cm and were either fixed in 4% neutral buffered formaldehyde for histologic assessment or collected in TRIzol or PBS for molecular analysis.

Immunohistochemical analysis

Immunocytochemistry on cell populations and IHC on formalin-fixed paraffin-embedded tissue sections were performed as described by Janzen and colleagues (30) with indicated antibodies and were imaged on an Olympus IX81 upright microscope equipped with cooled CCD camera and Image Pro-Plus software (Media Cybernetics). For histopathologic analysis, tissue sections (5 μm) were stained with hematoxylin and eosin.

String analysis

Protein–protein interactions were predicted using the Search Tool for the Retrieval of Interacting Genes/Proteins (STRING) database v 9.1 (http://www.string-db.org/). Proteins were linked based on the following six criteria; neighborhood, gene fusion, co-occurrence, co-expression, experimental evidence, and existing databases (31).

Statistical analysis

Statistical analysis was performed using two tailed-paired *t* test and one-way ANOVA with *post hoc* Tukey by GraphPad Prism (version 5.0). *P* values of <0.05 were considered statistically significant.

Results

Differential expression of functional ABC transporter ABCG2/Bcrp1 in cervical cancer cells

Flow cytometric analysis was done in different cervical cancer cell lines for expression of stemness marker, ABCG2, and identification of cervical CSCs. It revealed a major population of cells with variable expression of ABCG2 in all cells tested (Fig. 1A). The proportion of ABCG2-expressing cells was significantly higher in HPV^+ cells (SiHa, 94.3%; HeLa, 82.7%) as compared with that of HPV^- cells (C33a, 26.4%). Immunobloting also reconfirmed high level of ABCG2 expression in HPV^+ cells (Fig. 1B). To assess its functional relevance, cells were stained with DCV in absence or presence of ABCG2 inhibitor FTC. Mouse bone marrow cells used as positive control demonstrated a higher proportion of FTC-sensitive cancer stem-like cells and were designated as side population (SP; Fig. 1D). Cumulative analysis of cells in SP compartment demonstrated proportionally a higher percentage of SP in HPV^+ SiHa and HeLa cells as compared with HPV^- C33a cells (Fig. 1E).

Functional and molecular characterization of SP cells represents a distinct group of putative CaCxSLCs that selectively overexpress HPVE6 oncoprotein

In vitro sphere-forming ability of sorted SP and NSP cells were assessed for different days and the cervicospheres formed were

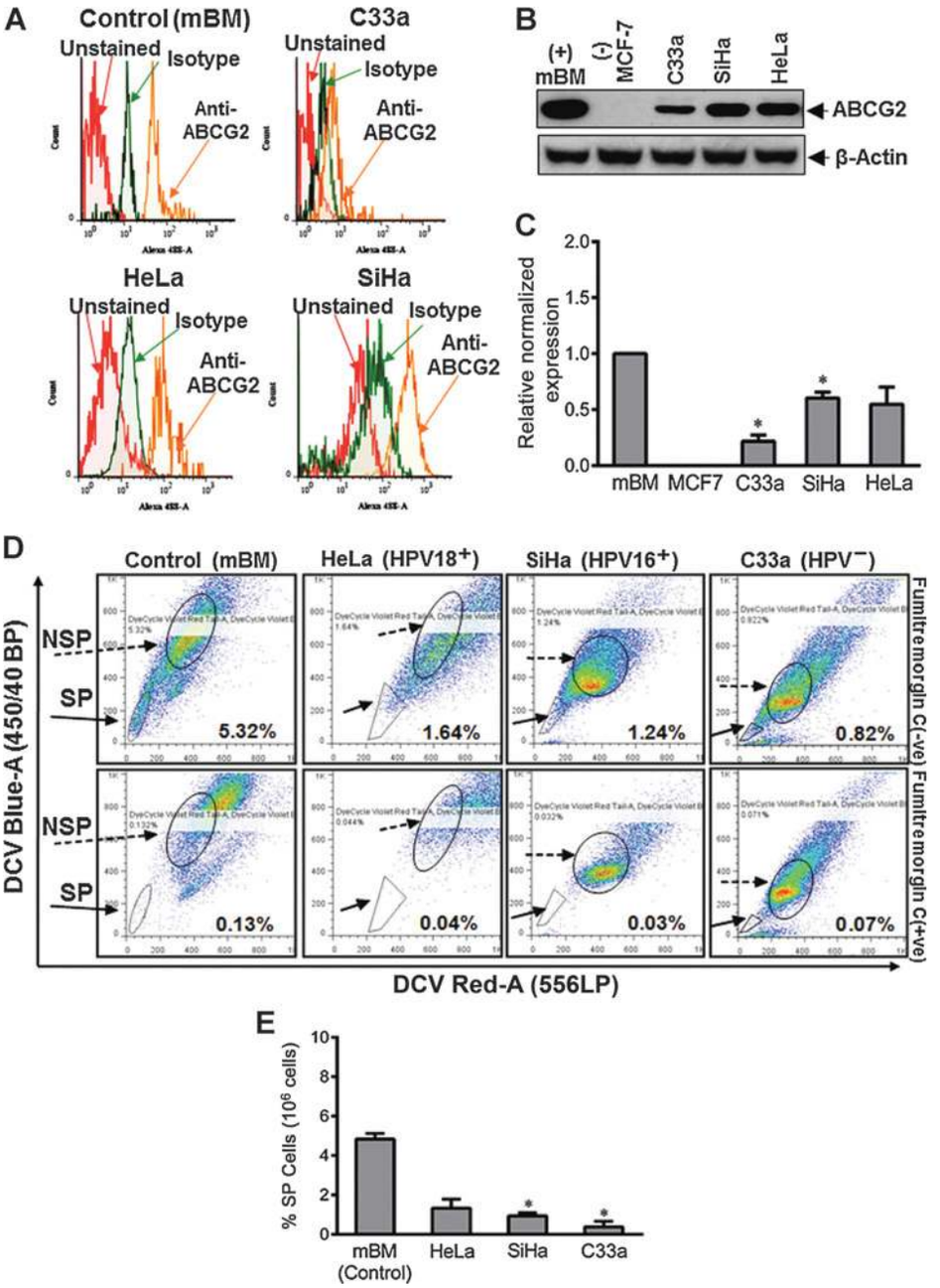

Figure 1.
Analysis of expression and function of stem cell marker ABCG2 in cervical cancer cells. **A,** phenotypic distribution of ABCG2 in cervical cancer cells. Flow cytometric analysis of ABCG2 protein expression in C33a, HeLa, and SiHa cells stained with ABCG2 antibody (orange). Unstained cells (red) were used as negative control. Mouse bone marrow cells (mBM) were used as positive control. **B,** representative immunoblot showing overall expression of ABCG2 in cervical cancer cell lines C33a, Hela, and SiHa. mBM and MCF-7 cells were used as positive and negative control, whereas β-actin was used a loading control. The abundance ratio of ABCG2 level to β-actin was analyzed by densitometry. **C,** normalized ABCG2 expression in different cell types expressed as mean ± SD of three independent experiments, *, P <0.05 versus C33a cells. **D,** functional distribution of ABCG2 in cervical cells. SP analysis of different cervical cancer cell lines by DCV exclusion method to determine the proportion of cells expressing functional ABCG2. Flow cytometric analyses of DCV-stained cells were analyzed in the absence or presence of Fumitremorgin C (FTC) showing FTC-sensitive, DCV-low cells designated as SP cells. **E,** cumulative data on three independent experiments showing percent SP cells (mean ± SD).*, $P < 0.05$ versus percent SP cells in C33a.

counted and molecularly characterized (see Supplementary Fig. 2S1). SP cells formed a good number of primary cervicospheres by day 10 in SiHa and HeLa (Fig. 2A). This duration was found optimal in our laboratory and was followed in all subsequent cervicosphere formation assays. Interestingly, neither C33a-SP cells nor NSP cells cultured in DCM could grow into cervicospheres but showed features of senescence/growth arrest. When we cultured the NSP cells in complete medium (CM), these cells failed to form cervicosphere and grew slowly as adherent monolayer. SiHa-SP cells formed a high degree of spheres which were distinctly larger than those observed in HeLa-SP cells (Fig. 2B) with SFE (SiHa, 0.3%; 0.13% in HeLa-0.13%). To examine the clonogenicity and self-renewability of cervicospheres, the primary cervicospheres from SP and NSP cultures were enzymatically dissociated into single-cell suspension and again cultured in respective DCM and CM at lower cell densities (2×10^3 cells/well) for 10 days. Cultures examined for secondary cervicosphere revealed a relatively increased sphere formation in SiHa-SP and HeLa SP cell cultures (Fig. 2C) with an increased SFE (SiHa, 0.75%; HeLa, 0.43%). Although there were some occasional small cervicospheres in NSP secondary cultures, they barely reached the threshold of counting. Secondary cervicospheres were examined for expression of Rb, p53, E6, E7, Lrig1, and Sox2 by immunoblotting and the level of pRB and Rb was much lower in NSP cells which showed a bit higher level of p53 (Fig. 2D). Furthermore, qRT-PCR of cDNA derived from SP and NSP cells demonstrated a

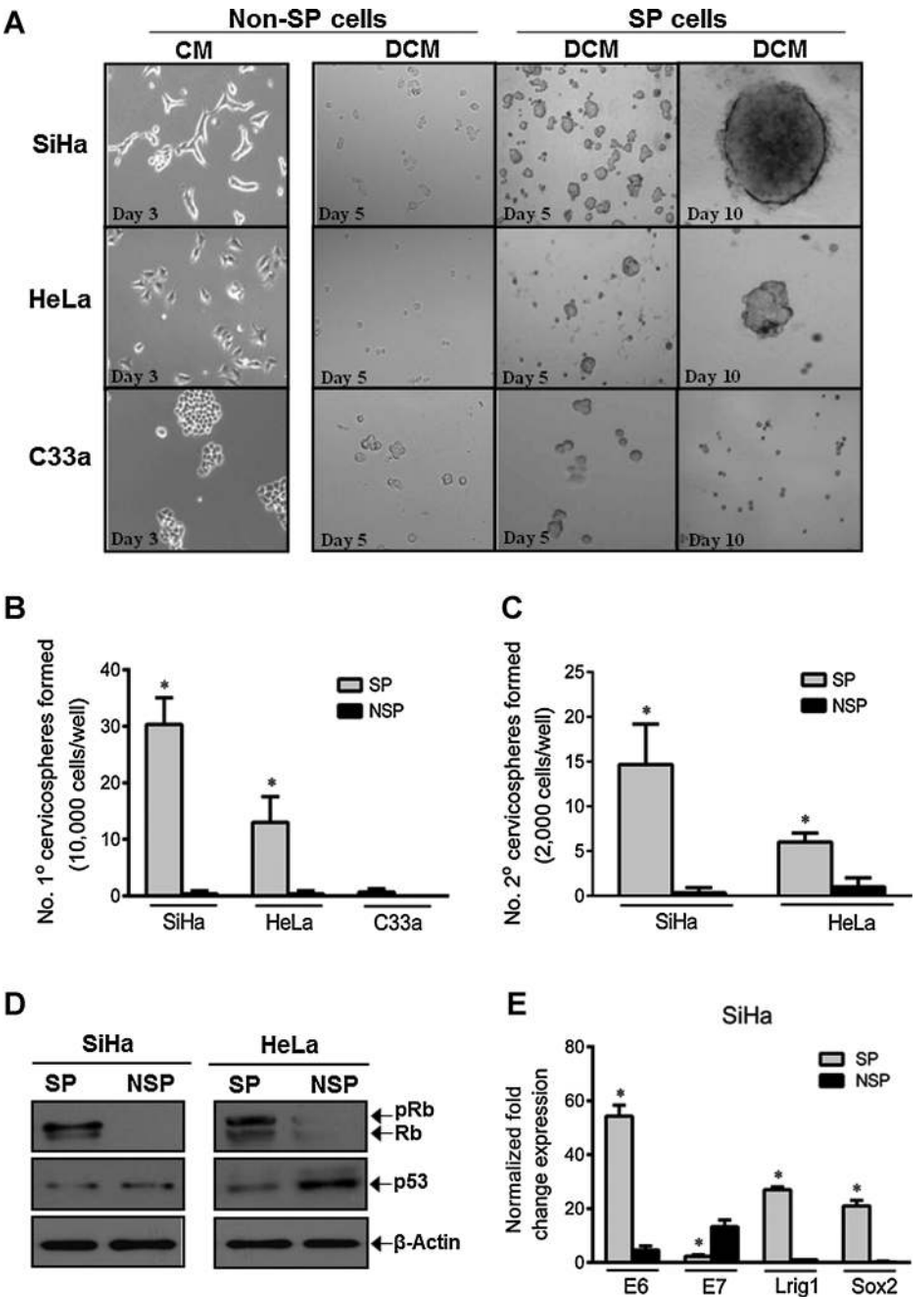

Figure 2.
Functional and molecular characterization of SP cells present in cervical cancer cells. **A,** assessment of cervicosphere-forming ability of SP cells. Representative photomicrograph of cervicosphere formation with sorted SP and non-SP cells in low adherence DCM (magnification, 100×). Cervicospheres were examined at day 3 and 7 and enumerated at day 10. Non-SP was seeded parallely in complete media (CM) with 10% FCS as reference. **B,** cumulative primary cervicosphere frequency (mean ± SD) in 10-day culture of SP and non-SP cells (seeding density, 1×10^4 cells/well) of three independent experiments. SiHa-SFE, 0.3%; HeLa-SFE, 0.13%. *, $P < 0.05$ versus SP cultures of C33a cells. **C,** frequencies (mean ± SD) of secondary (2°) cervicospheres formed from enzymatically dissociated cells from primary (1°) cervicospheres seeded with a cell density of 2×10^3 cells/well (SiHa-SFE, 0.75%; HeLa-SFE, 0.43%) in three independent experiments. *, $P < 0.05$ versus NSP cultures. **D,** expression pattern of pRb, Rb, and p53 in SP and non-SP cells. Representative immunoblots showing expression level of p53 and Rb/pRb in day 10 secondary cervicosphere cultures prepared from cells (2,000 cells/well) obtained from postenzymatic dissociation of primary cervicosphere cultures of SP and NSP cells. β-Actin was used as input control. **E,** transcript level of quiescence and pluripotency markers (Lrig1, Sox2) and viral oncogenes (E6 and E7) in cultures of SP and non-SP lineage. cDNA prepared from SP and non-SP cultures were analyzed by qRT-PCR for indicated transcripts. Unsorted SiHa cells were used as control and GAPDH was used as input control for normalization as described in Materials and Methods. The relative normalized fold change in transcript levels is expressed as mean ± SD of three independent experiments. *, $P < 0.05$ versus NSP cells.

slightly increased level of E6 and E7 transcripts, respectively, as compared with the control parental cells. SP cells, on the other hand, characteristically overexpressed E6, whereas E7 transcripts were relatively high in NSP cells. Cervicospheres from secondary SP cultures which showed higher expression of E6 also revealed higher expression of Lrig1 and Sox2 (Fig. 2E).

SP cervicospheres overexpressing HPVE6 show active Notch1 signaling

Next, we examined expression and DNA-binding activity of Notch1 along with its downstream gene associated with stemness, Hes1, in SP cervicosphere and NSP cells (see Supplementary Fig. 3S1). Parental SiHa or HeLa cells were used as controls. Immunoblotting using Notch1/Hes1 antibodies demonstrated lower expression of Notch1 but higher expression of Hes1 only in SP cells (Fig. 3A and B) while NSP cells lacked both Notch1 and Hes1 expression. To assess the DNA-binding activity of Notch1 that interact and facilitate CSL activation, nuclear protein from SP and NSP cells was subjected to CSL-specific EMSA using Hes1 gene promoter sequence that possesses a strong CSL-specific binding site upstream of TATA box (Fig. 3C). It showed a CSL-specific DNA-binding only in SP cells, whereas it was absent in NSP cells (Fig. 3D, ii). A supershift experiment with Notch1 (N1) antibodies demonstrated supershifted CSL-bands indicating an active involvement of Notch1 (Fig. 3D, iii). Confocal microscopy with Notch1 and ABCG2-stained cervicosphere further revealed localization of active Notch1 in cells expressing high ABCG2 (Fig. 3E).

CaCxSLCs are highly tumorigenic and recapitulate primary tumor histology in athymic nude mice

To assess whether the cervicospheres generated by novel sequential gating of SiHa and HeLa cells (SP→$CD49f^{+}CD71^{-}$→$CD133^{+}$; CaCxSLCs) exhibit slow proliferation, express Nanog and Oct4 (see Supplementary Fig. S4), and retain tumorigenic potential, a nude mouse xenograft model was established (see Supplementary Fig. 4S1 and A; Supplementary Table S2). Five of six athymic nude mice injected with lower doses (20×10^3 cells) of CaCxSLCs developed solid tumors (~1.0 cm^3) within three to four weeks (Fig. 4B). In contrast, mice with parental or non-CaCxSLCs showed no tumor formation with the same doses (Fig. 4B). Interestingly, a higher dose of parental tumor cells (0.5×10^6 cells) could form tumors (3/6; Fig. 4B). The CaCxSLC-derived tumors were found to grow faster and showed significantly an enhanced tumor burden as compared with parental tumors even at higher doses (Fig. 4C, i and ii). qRT-PCR analysis (Fig. 4D, i and ii) of these tumors demonstrated increased level of HPVE6, Hes1, ABCG2, and CD133 transcripts as compared with parental tumors. Histopathologic analysis of tumors showed epithelial origin and were morphologically similar to primary cervical tumor tissue (Fig. 4E). IHC of CaCxSLC tumors demonstrated enhanced positivity for Ki67, Hes1, ABCG2, and CD133 when compared with parental tumors but similar to primary cervical tumors (Fig. 4E).

To validate the above findings, we have established primary tissue cultures from human tissue specimens of cervical cancer patients ($n = 10$) to sort pCaCxSLCs by sequential triple gating (Fig. 4A and F) and subcutaneously injected at a dose of 0.1×10^6 cells in athymic nude mice ($n = 6$, Supplementary Table S2; Fig. 4G). After 4 weeks, pCaCxSLCs developed tumor (~1.0 cm^3) in 3 of 6 nu/nu mice (50%), whereas CaCxSLCs cells formed tumor in 4 of 6 nu/nu mice (66.6%; Fig. 4G, i and ii; Supplementary Table S2). Hematoxylin and eosin (H&E) staining of tissue sections from both the tumors (pCaCxSLCs and CaCxSLCs) showed their epithelial origin and histopathologically resembled primary tumors (Fig. 4H). Furthermore, IHC and immunoblotting of these tumors also showed enhanced staining of Ki67, Hes1, and ABCG2 (Fig. 4H) and significantly a higher expression for HPVE6 and Hes1 and a lower expression of Notch1 (Fig. 4I, i and ii). Interestingly, all these cell populations showed low expression of HPVE7 as expected.

Silencing of either HPV16E6 or Hes1 by specific siRNA in CaCxSLCs reduced expression of E6/Hes1, c-Fos/c-Jun/STAT3 leading to abolition of sphere forming and/or self-renewal ability

We examined the effect of HPV16E6 silencing by its specific siRNA on Notch1 and Hes1 expression and the sphere-forming ability of CaCxSLCs as shown in Supplementary Fig. S5S1. The qRT-PCR analysis of cDNA from siRNA-transfected cervicosphere cells revealed upto 80% loss of E6 transcripts (Fig. 5A). Although these cells did not show any significant change in Notch1 expression, Hes1 expression was significantly reduced and this was accompanied by reduced level of E6 and Hes1 proteins (Fig. 5B). CaCxSLCs treated with scrambled-siRNA only formed cervicosphere by day 10 while E6-siRNA–transfected cultures failed to form cervicospheres and showed cells spreading and underwent redifferentiation (Fig. 5C). As E6 silencing reduced Hes1 expression and resulted in loss of sphere formation, we then examined effect of Hes1 silencing on CaCxSLCs. It showed only approximately 40% loss of E6 expression but complete silencing of Hes1 expression (Fig. 5D and E) and approximately 75% loss of sphere-forming ability and partial induction of redifferentiation (Fig. 5F). This was also accompanied by about 60% reduction in Nanog expression (Fig. 5D). Furthermore, to dissect the signaling pathways and mechanism(s) involved, we did STRING database analysis to identify possible interacting proteins in parental, CaCxSLCs, or pCaCxSLCs cells and interestingly it revealed involvement of STAT3, pSTAT3, cJun, and cFos including E6 and Hes1 (Fig. 5G), but following Hes1 silencing, all of the above proteins were highly reduced with significant loss of sphere-forming ability in dose-dependent manner (Fig. 5H, i and ii).

Discussion

The study demonstrates for the first time higher expression of HPV oncoprotein E6 specifically in stem-like cells isolated from primary cervical tumor tissue or cancer cell lines and xenografts derived from them. Transient silencing of E6 strongly compromised their sphere-forming efficiency and blocked expression of Hes-1, a downstream gene of Notch1 responsible for stemness.

The identification of uterine cervical epithelial stem cells has been reported in cervical lesions and cancer cell lines (9, 10); these studies, however, did not elucidate the role of HPV, an essential etiologic agent for the development of cervical cancer, particularly in exacerbating malignant progression and stemness properties.

Of different approaches, the identification and isolation of CSCs with ABCG2 receptor, a major determinant of stemness (32), was found to be optimal and the expression of ABCG2 was significantly higher in CSCs that were positive for HPV. However,

ABCG2 overexpression was further assessed by measuring the active efflux of its specific fluorescent substrate, DCV, in presence/absence of FTC (33). We observed a much higher proportion of FTC-sensitive SP population mainly in HPV^+ cells than the HPV^- cells where the SP cells were barely detectable. This is in concordance with the earlier report (34). Furthermore, we observed that HPV^+ SP cells effectively formed cervicospheres, a hallmark feature of stemness and self-renewal capacity (35) but HPV^- SP cells (C33a) failed to form cervicospheres. We therefore suggest that a higher proportion of cells with stem cell property and higher sphere-forming ability may be attributed to the presence of HPV. Our hypothesis gains further support from the observations that viral infection and/or viral oncogenes can induce stem cell–like phenotype in human keratinocytes/epithelial cells by interfering with their differentiation (36).

Apart from ABCG2-based SP analysis, we also examined epithelial stem cell markers CD49f and CD71 (37) for isolation and enrichment (see Supplementary Fig. S3). However, except SiHa cells sorted only with $CD49f^+CD71^-$ phenotype failed to show any specific change of SFE (see Supplementary Fig. S2). These findings were suggestive of their lower applicability as a primary marker over ABCG2 in isolation of CaCxSLCs.

In contrast, we observed a gradual increase in SFE in secondary cervicosphere by employing serial passaging along with gating and sorting of cells, for SP phenotype followed by gating of cells on $CD49f^+CD71^-$ phenotype suggesting a potential utility of $CD49f^+CD71^-$ as secondary marker for enrichment of CaCxSLCs (see Supplementary Fig. S3). Serial passaging of sphere-forming cells helped in assessing their self-renewal capacity and intratumoral heterogeneity, thus mimicking both initiation and maintenance of tumors *in vivo* (38). Recently, similar approach involving serial passaging of cervical CSCs showed an increased SFE (10) but as they have not used stem cell markers at each passage, the increase in SFE was only marginal. Therefore, the sequential gating with sorting and reculturing of stem cells at each stage done by us proved to be a better strategy for enriching the CaCxSLCs. By incorporating CD133 as a marker for tertiary gating further increased

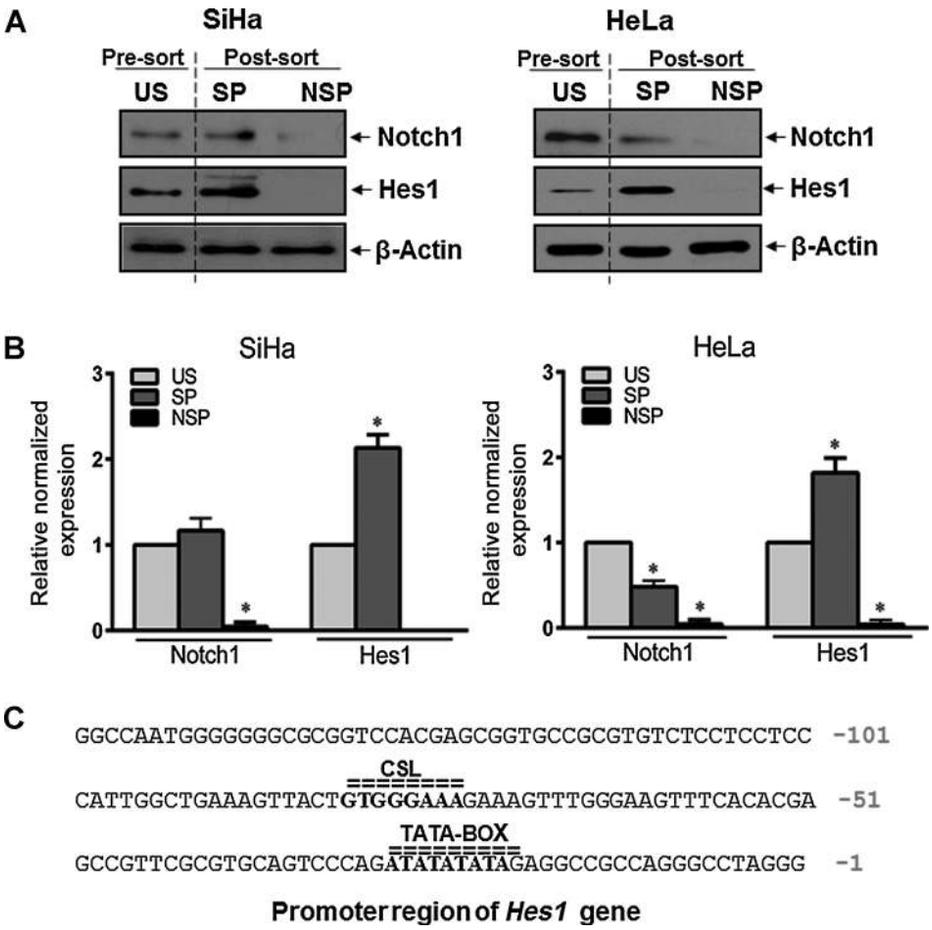

Figure 3.

Active Notch signaling in cervicospheres. **A,** representative immunoblot showing expression levels of Notch1, and its downstream protein, Hes1, in secondary cervicosphere cultures prepared from primary cervicosphere of SP and non-SP cultures. Presorted SiHa and HeLa cells were used as control (US). The abundance ratio of Notch1 and Hes1 protein to input control β-actin was analyzed by densitometry. **B,** the relative normalized fold change in the protein is expressed as the mean ± SD of three independent experiments. *, $P < 0.05$ versus parental presorted cells. **C,** nuclear Notch1 promotes CSL DNA-binding that controls Hes1 expression.Hes1 gene promoter sequence containing CSL-specific binding site at −81 to −74 position (in bold). (*Continued on the following page.*)

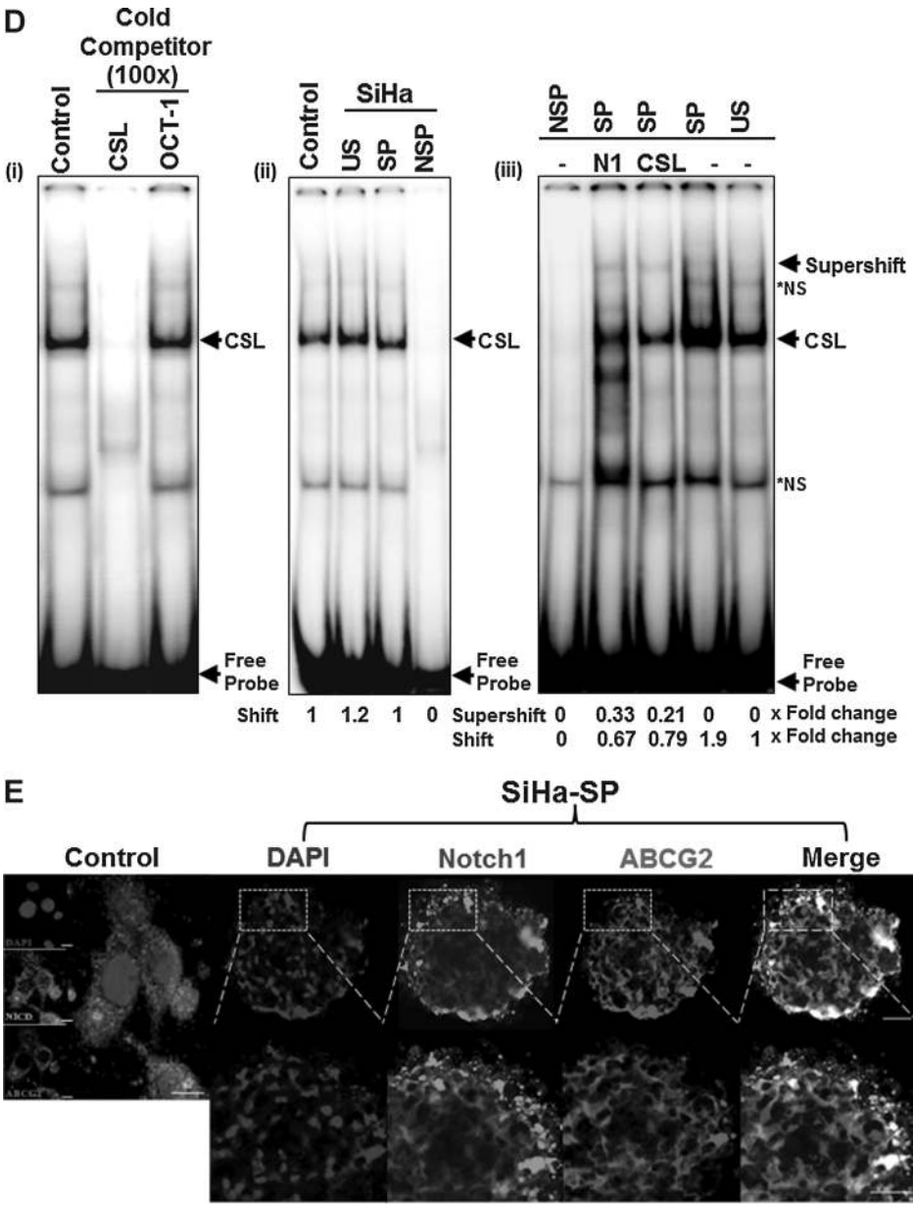

Figure 3.

(*Continued.*) **D,** representative radiograph showing CSL-specific DNA-binding activity in nuclear protein (10 μg/lane) derived from cells of the indicated culture at day 10. CSL-specific DNA-binding activity in nuclear protein was verified by cold competition as described in Materials and Methods (i). CSL-specific binding in nuclear proteins of cells in SP and non-SP cultures of SiHa cells (ii). Notch-specific supershift of CSL binding in nuclear proteins of SP and non-SP cells coincubated with Notch1(N1) or CSL-specific antibodies(CSL; iii). Marked arrow indicates the super-shifted band, respectively. *, NS, non-specific. **E,** correlative analysis of Notch1 expression with ABCG2 in cervicosphere. Representative confocal immunofluorescence image of ABCG2 and Notch1 in day 10 cultured secondary cervicospheres and parental SiHa cells (Scale bar = 50 μm). Each culture was fixed and stained with primary (ABCG2 and Notch1) and secondary antibodies [Alexa-488 (green) conjugated goat anti-mouse or Alexa-647 (red) conjugated donkey anti-goat antibodies] and counterstained with DAPI (blue) to visualize nuclei. White punctated stains in right panel represent colocalized ABCG2 and Notch1 in peripheral cells of cervicospheres.

the SFE but further passaging with any other marker did not increase the SFE (Supplementary Fig. S3).

It is interesting to note that there is relatively a lower level of endogenous p53 (as it binds to E6 and gets degraded by proteasome-mediated pathway) and a higher level of phosphorylated Rb detected in cervicosphere cells (see Fig. 2D). For continued cell proliferation and DNA replication, Rb remained phosphorylated and inactive or may bind to E7 while E2F remained free to reactivate cells to enter S-phase and enhanced cell proliferation. We also observed an increased E7 expression in NSP cells that were differentiated while E6 was highly expressed specifically in undifferentiated CaCxSLCs (see Fig. 2D). Thus, cervicospheres with stronger E6 expression but weaker E7 could well be correlated with the level of p53 and pRb in SP cells. Alterations in the level of

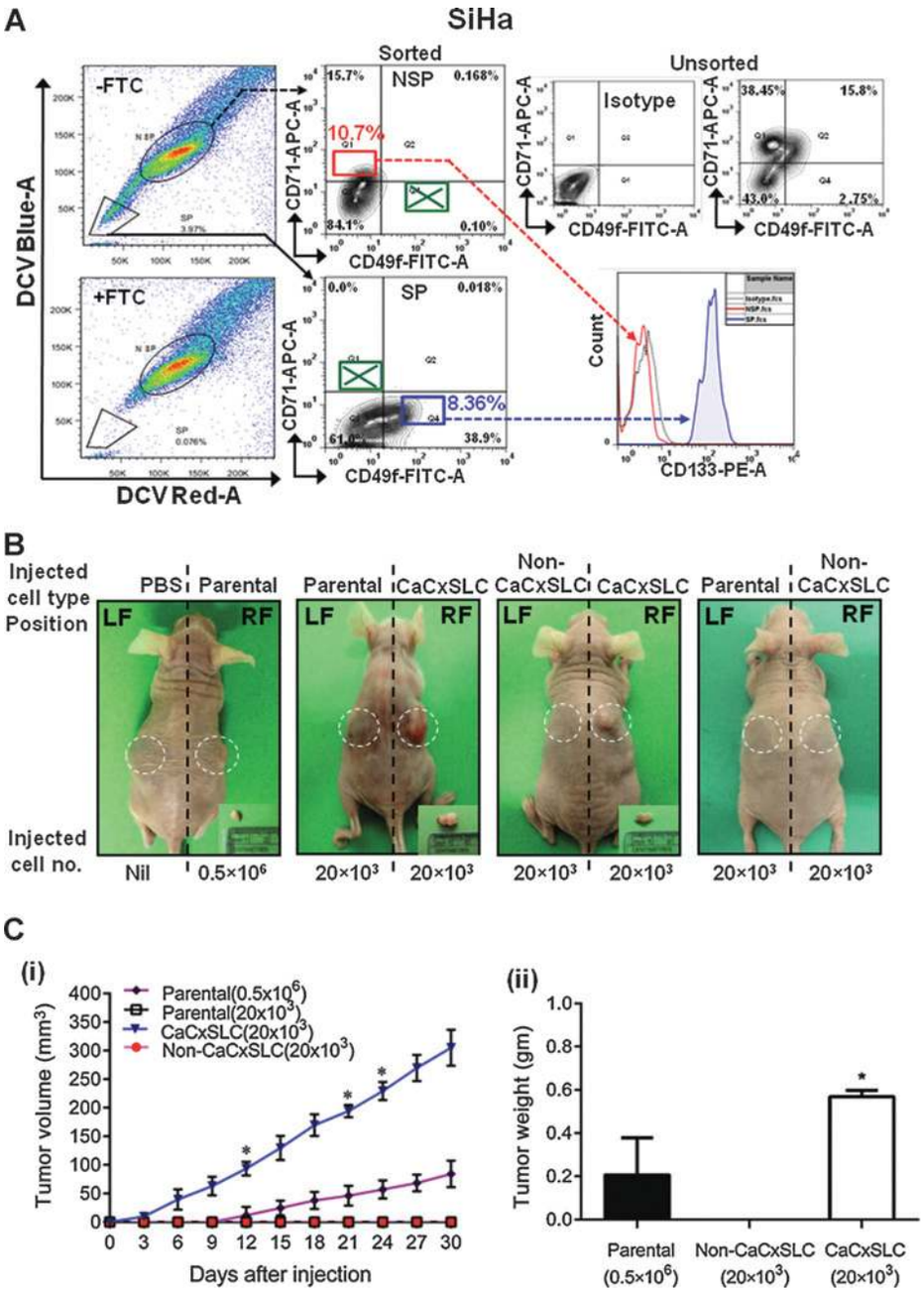

Figure 4.

CaCxSLCs cells from primary tumor tissue and cancer cell lines show *in vivo* tumorigenicity and were histologically similar to original primary tumor. **A,** representative flow cytometric analysis of parental and CaCxSLCs or non-CaCxSLCs cells isolated by sequential triple gating SP→CD49fCD71→CD133 as described in Materials and Methods. **B,** representative photographs of athymic nude mice transplanted with parental (20×10^3; 0.5×10^6) or CaCxSLC/non-CaCxSLC (20×10^3 each) cells obtained from SiHa cultures. **C,** tumor growth curves of parental (20×10^3; 0.5×10^6) or CaCxSLC/non-CaCxSLC (20×10^3 each) cells at 4 weeks postinjection in the athymic nude mice. Data presented as the mean ± SE; *, $P < 0.05$ versus parental tumor (i). Tumor weight derived from parental (0.5×10^6) or sorted CaCxSLCs (20×10^3) was measured after 4 weeks postinjection in the athymic nude mice. Data presented as mean ± SE; *, $P < 0.05$ versus parental tumor (ii). (*Continued on the following page.*)

E6 and E7 transcripts in stem versus non-stem cancer cells are suggestive of a highly dynamic HPV-regulated homeostatic mechanism that could be responsible for regulation of stemness. How and why this switching takes place from E7-predominated expression to E6-predominated expression in cervicospheres is not known. However, it is quite likely that factors governing alternate splicing of HPV's bicistronic transcripts that harbor both E6 and E7 mRNA might play a significant role (39). Collectively, these

results indicate that by altering the relative proportions of E6/E7 transcripts, HPV might alter the fate of cervical CSCs or vice versa. Thus, E7-overexpressing cells might be representing the bulk of differentiating tumor cells while E6 is responsible for undifferentiated state of cervical CSCs by enhancing the stemness properties. This is what exactly is shown recently by Lee and colleagues (40) in HPV$^-$ oral squamous cell carcinoma (OSCC) cells. After introduction of whole genome of HPV into these HPV$^-$ cells, it increased tumorigenicity in OSCC by enhancing the stemness through downregulation of specific miRNA. However, these investigators did not examine whether the effect was due to E6 or E7 expression.

Further analysis of cervicospheres revealed a higher expression of Lrig1 and Sox2. Lrig1 being a quiescence marker, cervicospheres were slow growing and the majority of cells were in G_0–G_1 phase of the cell cycle. This may be due to low metabolic activity or homeostatic balance (41). Similarly, a higher expression of Sox2, Oct4, and Nanog that contribute to pluripotency and self-renewal

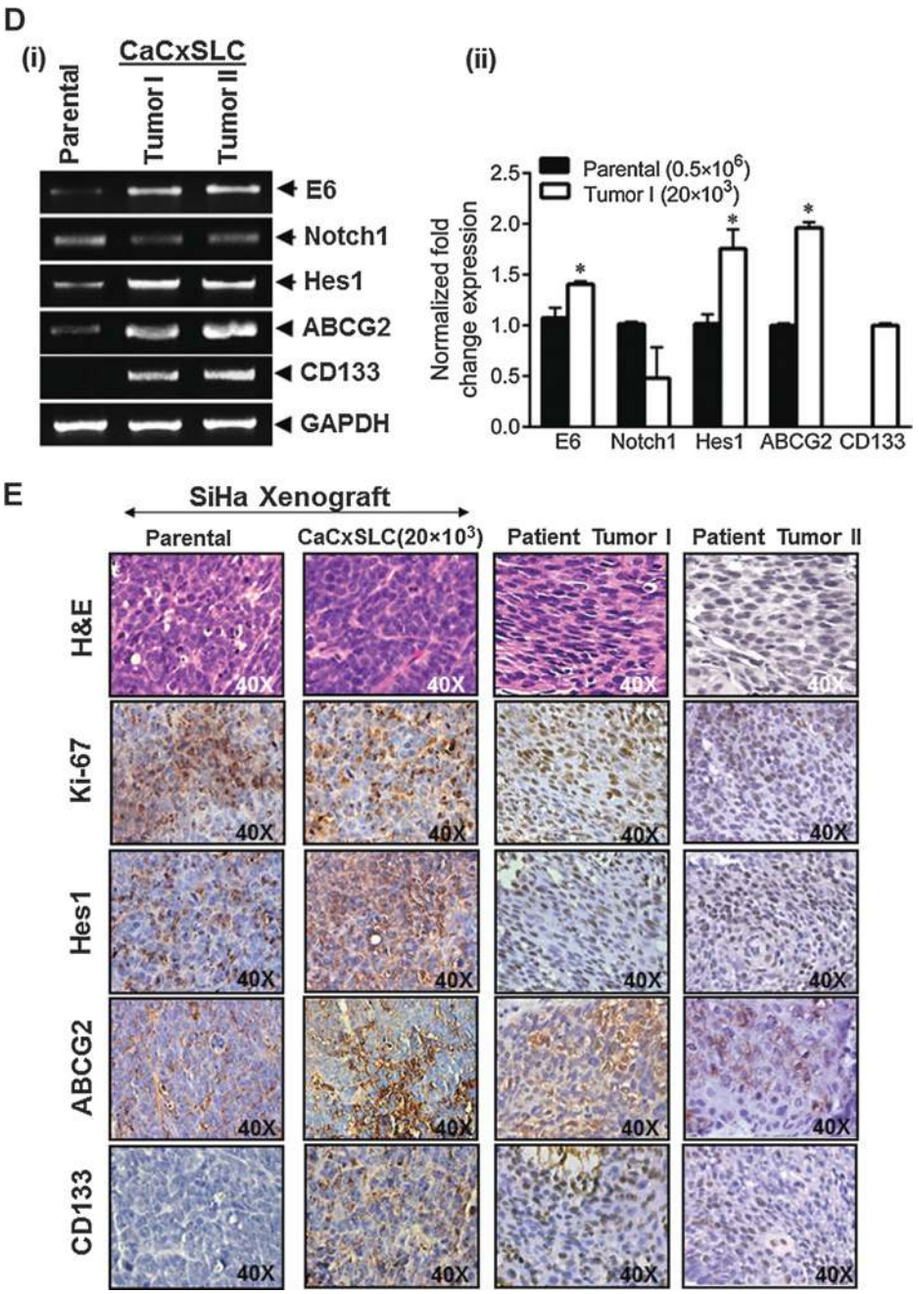

Figure 4.

(*Continued.*) **D,** qRT-PCR analysis of HPV16E6, Notch1, Hes1, ABCG2, and CD133 transcripts in tumors derived from parental or CaCxSLC cells (i). GAPDH was used as input control. Normalized fold change in transcript level is expressed as mean ± SD (ii). **E,** H&E staining and IHC of tumors derived from parental or CaCxSLC cells and tumor biopsies of cervical cancer patients (T1, T2; magnification, 400×). (*Continued on the following page.*)

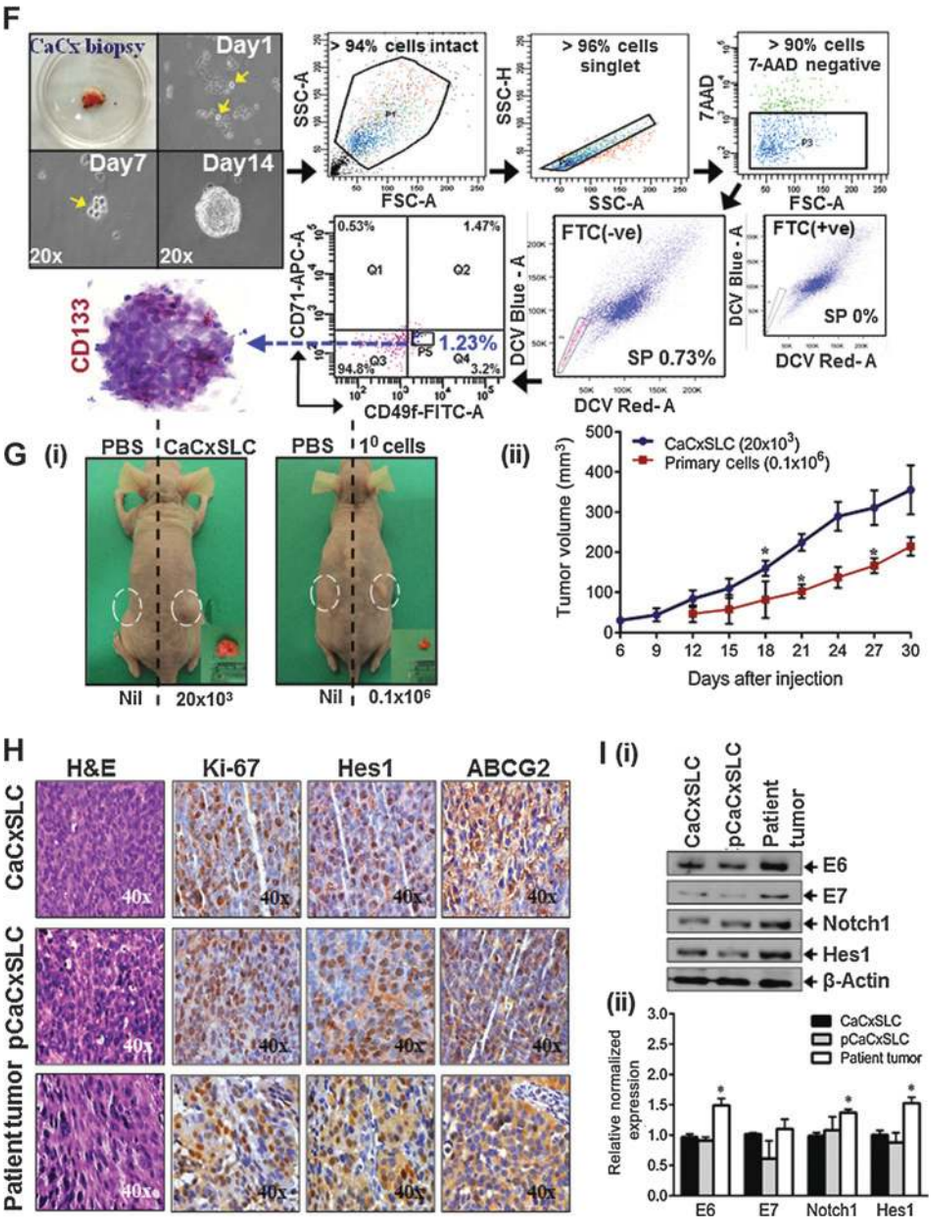

Figure 4.

(*Continued.*) **F,** representative flow cytometric analysis of primary tumor–derived pCaCxSLCs cells isolated by sequential triple gating as described in Materials and Methods. **G,** representative photographs of athymic nude mice transplanted with pCaCxSLCs or CaCxSLCs (i). Tumor growth curves of CaCxSLCs or pCaCxSLCs at 4 weeks post-injection in the athymic nude mice. Data presented as mean ± SD; *, $P < 0.05$ versus CaCxSLCs tumor (ii). **H,** H&E staining and representative IHC of tumor derived from pCaCxSLCs or CaCxSLCs and primary cervical tumor from patients (magnification, 400×). **I,** representative immunoblot showing expression levels of HPV16E6, E7, Notch1, and Hes1 proteins in tumors derived from pCaCxSLCs cells or CaCxSLCs cells and primary cervical tumor from patients (i). β-Actin was used as input control. The relative normalized fold change in the protein is expressed as the mean ± SD of three independent experiments; *, $P < 0.05$ vs. CaCxSLC tumor cells (ii).

(42) could be required for enhanced anchorage-independent growth (ref. 43; see Supplementary Fig. S4). Interestingly, the cellular morphology of xenograft tumors from pCaCxSLCs, CaCxSLCs, or parental cells and that of CINIII/IV cervical tumor (Fig. 4E and H) did show perfect similarity and recapitulated primary tumor histology and overexpressed HPV16E6, Hes1 and other stem cell markers. Collectively, these data provide unequivocal evidence in favor of an exclusive role of HPVE6 in CaCxSLCs. In addition, we assessed the proportion of CaCxSLCs in different stages of cervical cancer including the physical states of HPV. While the CINI/II lesions showed presence of mainly episomal viral DNA (80%; 4/5), 90% of CINIII/IV/cancer cases had either fully integrated (70%; 7/10) or mixed form (20%; 2/10) of HPV16 DNA. The xenografts obtained from primary culture of

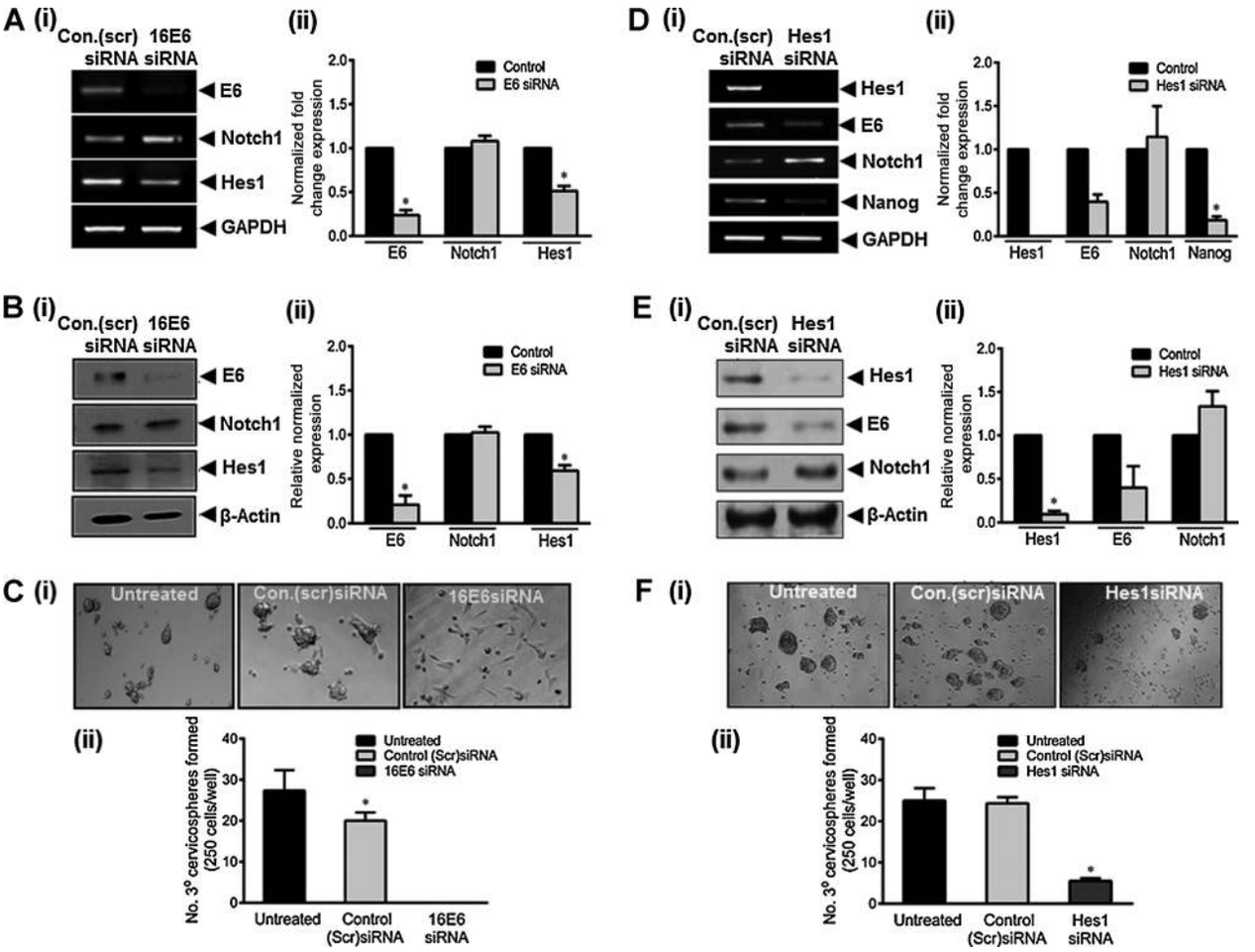

Figure 5.

Silencing of either HPV16 E6 or Hes1 in CaCxSLCs abrogates cervicosphere-forming ability. **A,** effect of E6 silencing in CaCxSLCs. Photomicrographs showing relative transcript levels of E6, Notch1, and Hes1 in CaCxSLC-transfected cells with E6-specific or control (scrambled) siRNA for 24 hours (i). GAPDH was used as input control for normalization as described in Materials and Methods. Normalized fold change in transcript levels is expressed as mean ± SD of three independent experiments; *, $P < 0.05$ versus CaCxSLCs treated with control siRNA (ii). **B,** representative immunoblots showing expression levels of E6, Notch1, and Hes1 in cells treated with E6-specific siRNA and control (scrambled) for 24 hours, respectively (i). β-Actin was used as control and the abundance ratio of each protein to β-actin was analyzed by densitometry. Relative normalized fold change in the protein is expressed as the mean ± SD of three independent experiments; *, $P < 0.05$ versus CaCxSLC treated with control siRNA (ii). **C,** representative photomicrograph of cervicospheres from CaCxSLCs transfected with E6-specific or control (scrambled) siRNA in DCM at day 10 (magnification, 100×; i). Frequencies of cervicospheres at day 10 formed in three independent experiments. Seeding density (250 cells/well). *, $P < 0.05$ versus untreated CaCxSLCs (ii). **D,** effect of Hes1 silencing on HPV16 E6, Notch1, and Nanog transcript levels in CaCxSLCs transfected with the E6-specific siRNA or control (scrambled) for 24 hours (i). Normalized fold change in transcript levels is expressed as mean ± SD of three independent experiments (ii). **E,** effect of Hes1 silencing on E6 and Notch1 protein levels in the cells treated with Hes1-specific siRNA and control (scrambled) for 24 hours, respectively (i). β-Actin was used as input control and the abundance ratio of each protein was analyzed by densitometry. Relative normalized expression of indicated protein expressed as the mean ± SD of three independent experiments (ii). **F,** cervicospheres from CaCxSLCs transfected with Hes1-specific siRNA and control (scrambled) in DCM at day 10 (magnification, 100×; i). Frequencies of cervicospheres at day 10 formed in three independent experiments. Seeding density (250 cells/well). *, $P < 0.05$ versus untreated CaCxSLCs (ii). (*Continued on the following page.*)

CINIII/IV cancer tissues showed almost all in integrated form (see Supplementary Table S3) which had higher proportion of CSCs as compared with those in CINI/II lesions with no characteristics of stemness and tumorigenicity (data not shown). This further strengthens our findings that HPV integration is essential for malignant progression and enhancement of stemness properties.

Notch signaling is known to regulate cell proliferation, differentiation, apoptosis, and stemness (15) and plays an important role in cervical carcinogenesis (44). HPV E6/E7 was found to upregulate Notch1 expression and activation of NICD (45); yet high Notch expression leads to growth arrest of these cells (13). Interestingly, we observed basal expression of Notch1 while overexpression of Hes1 in HPVE6-overexpressing cervicospheres but it was completely absent in NSP cells. In addition, cervicospheres showed active Notch1 on Hes1 promoter in CSL-dependent manner followed by colocalization with ABCG2. Collectively, these observations indicate that Notch1 expression in cervicosphere might contribute to stemness and anchorage-independent

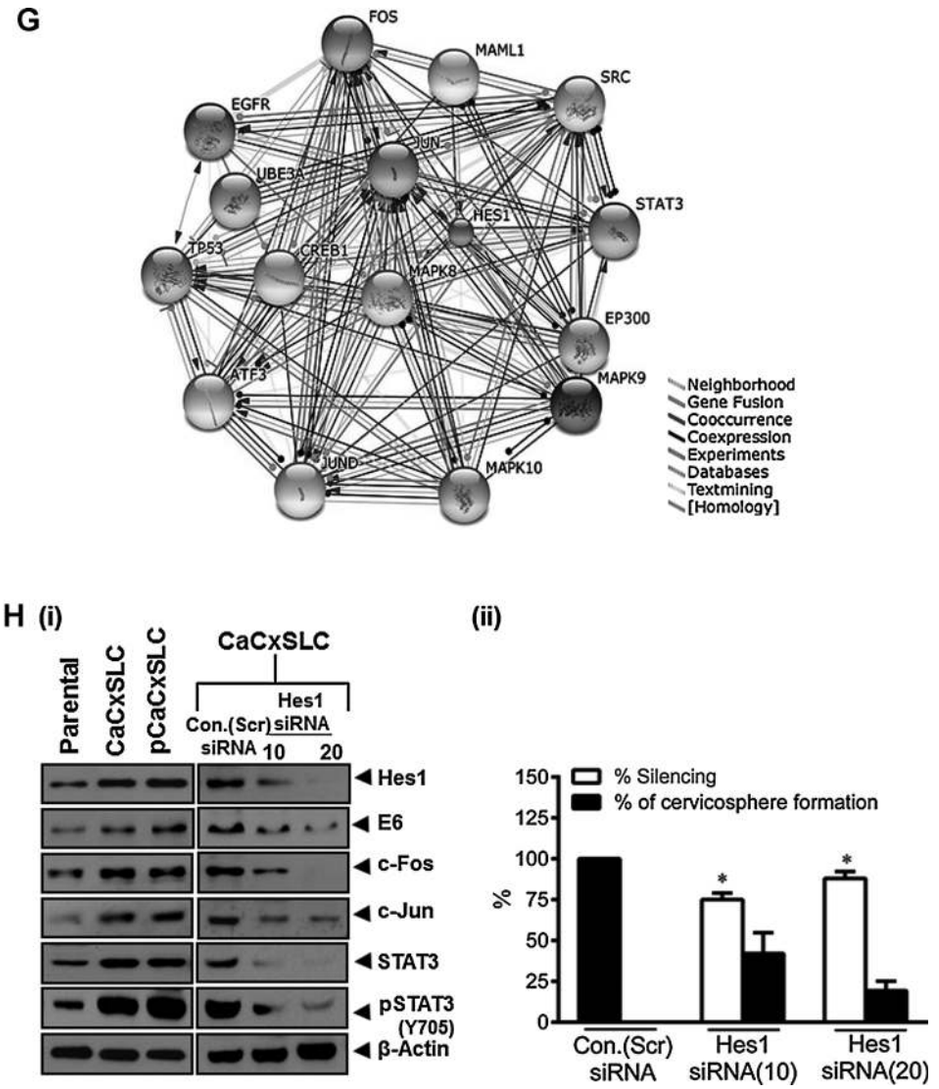

Figure 5.
(*Continued.*) **G,** STRING database analysis for cancer-associated protein–protein interactions network on the basis of protein association of high confidence (score>0.7). **H,** representative immunoblots showing expression level of Hes1, cFos, cJun, E6, STAT3, pSTAT3 in parental, CaCxSLCs, or pCaCxSLCs cells. β-Actin was used as input control. The abundance ratio of each protein to β-actin was analyzed by densitometry (i). Relative normalized fold change in the protein is expressed as the mean ± SD of three independent experiments; *, $P < 0.05$ versus CaCxSLCs treated with Hes1-siRNA (ii). 3°, tertiary.

growth via ABCG2 and Hes1 upregulation as both are direct targets of Notch1 signaling (46).

To examine the role of HPVE6 in maintenance of CaCxSLCs, we silenced its expression by E6 siRNA. It is intriguing to note that although E6 silencing did not affect Notch1 expression to a great extent, it caused a significant (∼40%) loss in Hes1 expression, but the loss of E6 (∼80%) severely affected the sphere-forming ability of CaCxSLCs which underwent differentiation (see Fig. 5C, i). In contrast, when Hes1 was silenced, there was complete loss of Hes1 expression but E6 expression was only moderately affected (∼40%) and the sphere-forming ability was only partially affected (see Fig. 5F, i). These findings demonstrate an interesting cross talk between HPVE6 and Hes1 wherein E6 oncoprotein plays a critical role in regulation of stem cell phenotype including undifferentiated state and sphere-forming ability. Hes1 has been recently shown to desynchronize differentiation of pluripotent embryonic stem cells by modulating STAT3 signaling (47) which also plays a pivotal role in cervical carcinogenesis (22). The absence of significant effect of E6 or Hes1 silencing on Notch1 is suggestive of the fact that overexpression of Hes1 may not be absolutely dependent on Notch1 and could be regulated by other heterogeneously expressed transcription factors as reported earlier (48). Nevertheless, our study gains strong support from a recent report that showed existence of crosstalk between HPVE6 and Hes1 (49). To understand the possible mechanism(s) involved, we did STRING database analysis based on a series of reports from our laboratory and others on the role of AP-1 and STAT3 in cervical carcinogenesis (29, 50–52). It demonstrated that Fos/Jun/AP-1, STAT3, and Notch1 activate Hes1 as well as E6 expression through their functional interaction and involvement in transcription regulation, signal transduction, cell proliferation, differentiation, and maintenance of stemness in cervical CSCs. Further validation by expression of Fos/Jun/AP-1 and STAT3 key proteins clearly demonstrated an interactive crosstalk between Hes1 and E6 through Notch1–AP-1–STAT3 signaling pathways (see Fig. 5G–I). On this basis, we derived a model (Fig. 6) that show the primary mechanism(s) involved.

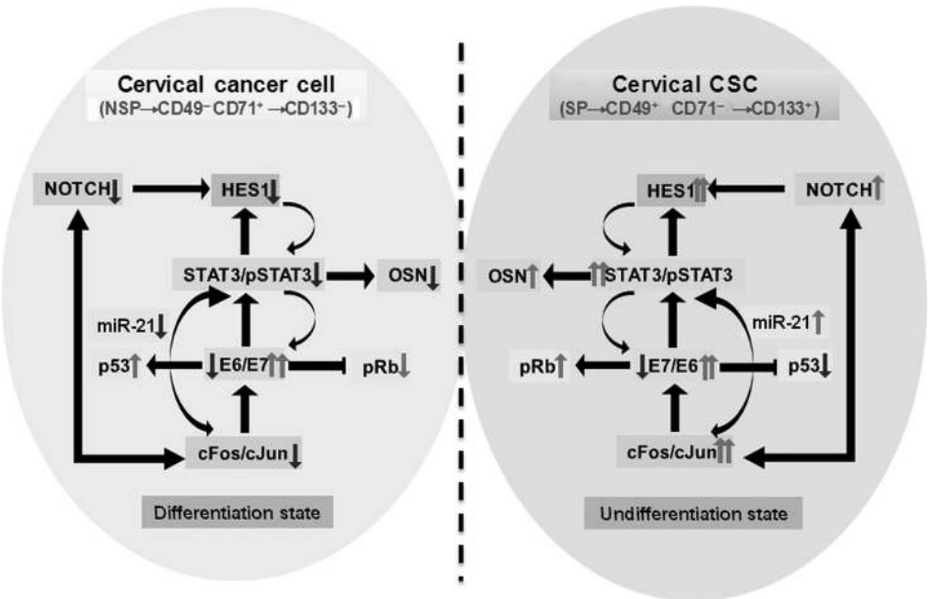

Figure 6.
Possible model showing involvement of signaling pathways Notch-AP-1 (Fos/Jun)-STAT3 in cervical cancer and CSCs.

In conclusion, we demonstrate for the first time an essential role of HPV oncoprotein E6 that selectively overexpresses in CaCxSLCs and participates in maintenance of stem cell phenotype and stemness through upregulation of Hes1 while preponderance of E7 leads to differentiation. In addition, a novel procedure has been developed for isolation and enrichment of cervical CSCs from cancer cell lines as well as from patient's tumors by sequential triple gating using cell-specific markers SP→($CD49f^{+}CD71^{-}$)→$CD133^{+}$ with intermittent culturing in low adhesion environment. As inhibition of E6 expression leads to loss of self-renewability/stemness of CSCs, it offers a unique opportunity in developing effective therapeutics for targeting the chemo-radioresistant CSCs.

Disclosure of Potential Conflicts of Interest

No potential conflicts of interest were disclosed.

Authors' Contributions

Conception and design: B.C. Das, A. Tyagi, A.C. Bharti
Development of methodology: B.C. Das, A. Tyagi, A.C. Bharti
Acquisition of data (provided animals, acquired and managed patients, provided facilities, etc.): B.C. Das, A. Tyagi, G. Verma, Y. Srivastava, B.G. Roy
Analysis and interpretation of data (e.g., statistical analysis, biostatistics, computational analysis): B.C. Das, A. Tyagi, K. Vishnoi, S. Mahata, G. Verma, Y. Srivastava, S. Masaldan, B.G. Roy, A.C. Bharti
Writing, review, and/or revision of the manuscript: B.C. Das, A. Tyagi, K. Vishnoi, G. Verma, A.C. Bharti
Administrative, technical, or material support (i.e., reporting or organizing data, constructing databases): B.C. Das, A.C. Bharti
Study supervision: B.C. Das

Grant Support

The study was supported by J. C. Bose grants from the Department of Science & Technology (DST; to B.C. Das) and by Indian Council of Medical Research [ICMR, Government of India; to B.C. Das and A.C. Bharti; ICMR Senior Research Fellowship; to A. Tyagi (grant no. 81/3/2009/BMS/Stem Cell)]. This study was also supported by grants from the CSIR-UGC [F.2-2/2009 (SA-I); to K. Vishnoi and G. Verma] and ICMR [3/1/13/PDF(2)/2011-HRD, to S. Mahata; and 50/1-1/TF/2012-NCDII, to S. Masaldan].

The costs of publication of this article were defrayed in part by the payment of page charges. This article must therefore be hereby marked *advertisement* in accordance with 18 U.S.C. Section 1734 solely to indicate this fact.

Received October 23, 2015; revised January 29, 2016; accepted February 19, 2016; published OnlineFirst March 17, 2016.

References

1. zur Hausen H.Papillomaviruses and cancer: from basic studies to clinical application.Nat Rev Cancer 2002;2:342–50.
2. Das BC, Sehgal A, Murthy NS, Gopalkrishna V, Sharma JK, Das DK, et al. Human papillomavirus and cervical cancer in Indian women. Lancet 1989;2:1271.
3. Das BC, Hussain S, Nasare V, Bharadwaj M. Prospects and prejudices of human papillomavirus vaccines in India. Vaccine 2008;26:2669–79.
4. Pectasides D, Kamposioras K, Papaxoinis G, Pectasides E. Chemotherapy for recurrent cervical cancer. Cancer Treat Rev 2008;34:603–13.
5. Ho GY, Burk RD, Klein S, Kadish AS, Chang CJ, Palan P, et al. Persistent genital human papillomavirus infection as a risk factor for persistent cervical dysplasia. J Natl Cancer Inst 1995;87:1365–71.
6. Wu W, Vieira J, Fiore N, Banerjee P, Sieburg M, Rochford R, et al. KSHV/HHV-8 infection of human hematopoietic progenitor (CD34+) cells: persistence of infection during hematopoiesis *invitro* and *invivo*. Blood 2006;108:141–51.
7. Martens JE, Arends J, Van der Linden PJ, De Boer BA, Helmerhorst TJ. Cytokeratin 17 and p63 are markers of the HPV target cell, the cervical stem cell. Anticancer Res 2004;24:771–5.
8. Herfs M, Yamamoto Y, Laury A, Wang X, Nucci MR, McLaughlin-Drubin ME, et al. A discrete population of squamocolumnar junction cells implicated in the pathogenesis of cervical cancer. Proc Natl Acad Sci U S A 2012;109:10516–21.
9. Feng D, Peng C, Li C, Zhou Y, Li M, Ling B, et al. Identification and characterization of cancer stem-like cells from primary carcinoma of the cervix uteri. Oncol Rep 2009;22:1129–34.
10. Lopez J, Poitevin A, Mendoza-Martinez V, Perez-Plasencia C, Garcia-Carranca A. Cancer-initiating cells derived from established cervical cell

lines exhibit stem-cell markers and increased radioresistance. BMC Cancer 2012;12:48.
11. Dyson N, Howley PM, Munger K, Harlow E. The human papilloma virus-16 E7 oncoprotein is able to bind to the retinoblastoma gene product. Science 1989;243:934–7.
12. Werness BA, Levine AJ, Howley PM. Association of human papillomavirus types 16 and 18 E6 proteins with p53. Science 1990;248:76–9.
13. Talora C, Cialfi S, Segatto O, Morrone S, Kim Choi J, Frati L, et al. Constitutively active Notch1 induces growth arrest of HPV-positive cervical cancer cells via separate signaling pathways. Exp Cell Res 2005;305: 343–54.
14. Henken FE, De-Castro Arce J, Rosl F, Bosch L, Meijer CJ, Snijders PJ, et al. The functional role of Notch signaling in HPV-mediated transformation is dose-dependent and linked to AP-1 alterations. Cell Oncol 2012;35: 77–84.
15. Chiba S.Notch signaling in stem cell systems. Stem Cells 2006;24: 2437–47.
16. Jensen KB, Watt FM. Single-cell expression profiling of human epidermal stem and transit-amplifying cells: Lrig1 is a regulator of stem cell quiescence. Proc Natl Acad Sci U S A 2006;103:11958–63.
17. Turin I, Schiavo R, Maestri M, Luinetti O, Bello B, Paulli M, et al. In vitro efficient expansion of tumor cells deriving from different types of human tumor samples. Med Sci 2014;2:70–81.
18. Telford WG, Bradford J, Godfrey W, Robey RW, Bates SE. Side population analysis using a violet-excited cell-permeable DNA binding dye. Stem Cells 2007;25:1029–36.
19. Dontu G, Abdallah WM, Foley JM, Jackson KW, Clarke MF, Kawamura MJ, et al. *Invitro* propagation and transcriptional profiling of human mammary stem/progenitor cells. Genes Dev 2003;17:1253–70.
20. Dey D, Saxena M, Paranjape AN, Krishnan V, Giraddi R, Kumar MV, et al. Phenotypic and functional characterization of human mammary stem/ progenitor cells in long term culture. PLoS One 2009;4:e5329.
21. Shukla S, Mahata S, Shishodia G, Pande S, Verma G, Hedau S, et al. Physical state & copy number of high risk human papillomavirus type 16 DNA in progression of cervical cancer. Indian J Med Res 2014;139:531–43.
22. Shukla S, Shishodia G, Mahata S, Hedau S, Pandey A, Bhambhani S, et al. Aberrant expression and constitutive activation of STAT3 in cervical carcinogenesis: implications in high-risk human papillomavirus infection. Mol Cancer 2010;9:282.
23. Bharti AC, Donato N, Singh S, Aggarwal BB. Curcumin (diferuloylmethane) down-regulates the constitutive activation of nuclear factor-kappa B and IkappaBalpha kinase in human multiple myeloma cells, leading to suppression of proliferation and induction of apoptosis. Blood 2003;101:1053–62.
24. Katoh M. Integrative genomic analyses on HES/HEY family: Notch-independent HES1, HES3 transcription in undifferentiated ES cells, and Notch-dependent HES1, HES5, HEY1, HEY2, HEYL transcription in fetal tissues, adult tissues, or cancer. Int J Oncol 2007;31:461–6.
25. Weiswald LB, Guinebretiere JM, Richon S, Bellet D, Saubamea B, Dangles-Marie V. *Insitu* protein expression in tumour spheres: development of an immunostaining protocol for confocal microscopy. BMC Cancer 2010; 10:106.
26. Mosmann T. Rapid colorimetric assay for cellular growth and survival: application to proliferation and cytotoxicity assays. J Immunol Methods 1983;65:55–63.
27. Hamburger AW, Salmon SE. Primary bioassay of human tumor stem cells. Science 1977;197:461–3.
28. Debacq-Chainiaux F, Erusalimsky JD, Campisi J, Toussaint O. Protocols to detect senescence-associated beta-galactosidase (SA-betagal) activity, a biomarker of senescent cells in culture and *invivo*. Nat Protoc 2009;4: 1798–806.
29. Shukla S, Mahata S, Shishodia G, Pandey A, Tyagi A, Vishnoi K, et al. Functional regulatory role of STAT3 in HPV16-mediated cervical carcinogenesis. PLoS One 2013;8:e67849.
30. Janzen DM, Cheng D, Schafenacker AM, Paik DY, Goldstein AS, Witte ON, et al. Estrogen and progesterone together expand murine endometrial epithelial progenitor cells. Stem Cells 2013;31:808–22.
31. Franceschini A, Szklarczyk D, Frankild S, Kuhn M, Simonovic M, Roth A, et al. STRING v9.1: protein-protein interaction networks, with increased coverage and integration. Nucleic Acids Res 2013;41: D808–15.
32. Goodell MA, Brose K, Paradis G, Conner AS, Mulligan RC. Isolation and functional properties of murine hematopoietic stem cells that are replicating *in vivo*. J Exp Med 1996;183:1797–806.
33. Rabindran SK, Ross DD, Doyle LA, Yang W, Greenberger LM. Fumitremorgin C reverses multidrug resistance in cells transfected with the breast cancer resistance protein. Cancer Res 2000;60:47–50.
34. Villanueva-Toledo J, Ponciano-Gomez A, Ortiz-Sanchez E, Garrido E. Side populations from cervical-cancer-derived cell lines have stem-cell-like properties. Mol Biol Rep 2014;41:1993–2004.
35. Bruno L, Hoffmann R, McBlane F, Brown J, Gupta R, Joshi C, et al. Molecular signatures of self-renewal, differentiation, and lineage choice in multipotential hemopoietic progenitor cells *invitro*. Mol Cell Biol 2004;24:741–56.
36. Hufbauer M, Biddle A, Borgogna C, Gariglio M, Doorbar J, Storey A, et al. Expression of betapapillomavirus oncogenes increases the number of keratinocytes with stem cell-like properties. J Virol 2013;87:12158–65.
37. Li A, Pouliot N, Redvers R, Kaur P. Extensive tissue-regenerative capacity of neonatal human keratinocyte stem cells and their progeny. J Clin Invest 2004;113:390–400.
38. Patel SA, Ramkissoon SH, Bryan M, Pliner LF, Dontu G, Patel PS, et al. Delineation of breast cancer cell hierarchy identifies the subset responsible for dormancy. Sci Rep 2012;2:906.
39. Tan TM, Gloss B, Bernard HU, Ting RC. Mechanism of translation of the bicistronic mRNA encoding human papillomavirus type 16 E6-E7 genes. J Gen Virol 1994;75:2663–70.
40. Lee SH, Lee CR, Rigas NK, Kim RH, Kang MK, Park NH, et al. Human papillomavirus 16 (HPV16) enhances tumor growth and cancer stemness of HPV-negative oral/oropharyngeal squamous cell carcinoma cells via miR-181 regulation. Papillomavirus Res 2015;1:116–25.
41. Valcourt JR, Lemons JM, Haley EM, Kojima M, Demuren OO, Coller HA. Staying alive: metabolic adaptations to quiescence. Cell Cycle 2012;11: 1680–96.
42. Boyer LA, Lee TI, Cole MF, Johnstone SE, Levine SS, Zucker JP, et al. Core transcriptional regulatory circuitry in human embryonic stem cells. Cell 2005;122:947–56.
43. Ji J, Zheng PS. Expression of Sox2 in human cervical carcinogenesis. Hum Pathol 2010;41:1438–47.
44. Wang Z, Li Y, Sarkar FH. Notch signaling proteins: legitimate targets for cancer therapy. Curr Protein Pept Sci 2010;11:398–408.
45. Weijzen S, Zlobin A, Braid M, Miele L, Kast WM. HPV16 E6 and E7 oncoproteins regulate Notch-1 expression and cooperate to induce transformation. J Cell Physiol 2003;194:356–62.
46. Bhattacharya S, Das A, Mallya K, Ahmad I. Maintenance of retinal stem cells by Abcg2 is regulated by notch signaling. J Cell Sci 2007; 120:2652–62.
47. Zhou X, Smith AJ, Waterhouse A, Blin G, Malaguti M, Lin CY, et al. Hes1 desynchronizes differentiation of pluripotent cells by modulating STAT3 activity. Stem Cells 2013;31:1511–22.
48. Curry CL, Reed LL, Nickoloff BJ, Miele L, Foreman KE. Notch-independent regulation of Hes-1 expression by c-Jun N-terminal kinase signaling in human endothelial cells. Lab Invest 2006;86:842–52.
49. Vliet-Gregg PA, Hamilton JR, Katzenellenbogen RA. Human papillomavirus 16E6 and NFX1–123 potentiate Notch signaling and differentiation without activating cellular arrest. Virology 2015;478:50–60.
50. Ren C, Cheng X, Lu B, Yang G. Activation of interleukin-6/signal transducer and activator of transcription 3 by human papillomavirus early proteins 6 induces fibroblast senescence to promote cervical tumourigenesis through autocrine and paracrine pathways in tumour microenvironment. Eur J Cancer 2013;49:3889–99.
51. Rosl F, Das BC, Lengert M, Geletneky K, zur Hausen H. Antioxidant-induced changes of the AP-1 transcription complex are paralleled by a selective suppression of human papillomavirus transcription. J Virol 1997;71:362–70.
52. Prusty BK, Das BC. Constitutive activation of transcription factor AP-1 in cervical cancer and suppression of human papillomavirus (HPV) transcription and AP-1 activity in HeLa cells by curcumin. Int J Cancer 2005;113:951–60.